Characteristics of Cobalt Nanoneedles in 10% Co/Aerogel Fischer−Tropsch Catalyst

P. Dutta,[†] B. C. Dunn,[‡] E. M. Eyring,[‡] N. Shah,[§] G. P. Huffman,[§] A. Manivannan,[†] and M. S. Seehra*,[†]

Department of Physics, West Virginia University, Morgantown, West Virginia 26506, Department of Chemistry, University of Utah, Salt Lake City, Utah 84112, and College of Engineering, University of Kentucky, Lexington, Kentucky 40506

Received May 16, 2005. Revised Manuscript Received July 12, 2005

The 10% Co/aerogel catalyst used in Fischer−Tropsch (FT) synthesis recently by Dunn et al. (Dunn, B. C.; Cole, P.; Covington, D.; Webster, M. C.; Pugmire, R. J.; Ernst, R. D.; Eyring, E. M.; Shah, N.; Huffman, G. P. *Appl. Catal., A* **2005**, *278*, 233) is investigated using the complimentary techniques of X-ray diffraction (XRD), transmission electron microscopy (TEM), and detailed magnetic measurements. TEM studies show that the catalyst contains Co nanoneedles with diameter $d \approx 1$ nm, whereas the XRD studies show the presence of CoO and cobalt silicate hydroxide $Co_3(Si_2O_5)(OH)_2$, in addition to Co. Analysis of the temperature and magnetic field variation of the magnetization from 5 to 350 K shows that the measured magnetic properties are primarily due to the Co nanoneedles oriented randomly, with concentration ≈8%. The presence of the unreduced CoO and the Co silicate explains why the FT activity of this catalyst is about equal to that of the 6% Co/aerogel catalyst. Some interesting magnetic properties of the Co nanoneedles are also presented.

Introduction

In a recent paper,[1] Dunn et al. have reported the use of Co catalysts supported on silica aerogel (2, 6, and 10 wt % loading) for Fischer−Tropsch (FT) activity in a laboratory-scale packed-bed reactor. The percentages of CO conversion were found to be 5.3, 19.8, and 22.3% for the 2, 6, and 10% Co loading, respectively. One of the interesting features of the characteristics of these catalysts was that the morphology of the 10%Co loaded particles was distinctly different than the other catalysts. Whereas the particles of the 2 and 6% loadings were nearly spherical with diameters of about 50 and 70 nm, respectively, the 10% Co loading produced needlelike structures. Also, in temperature-programmed reduction (TPR), the 10% loading produced an additional peak near 680 °C, which was speculated to be due to Co−silicates, although the exact nature of the silicate was not determined. The fact that there is no significant increase in CO conversion in going from 6 to 10% Co loading also suggests a complex nature of the 10% Co/aerogel catalyst.

In this work, we have carried out detailed investigations of the 10%Co/aerogel catalyst using X-ray diffraction (XRD), transmission electron microscopy (TEM), and temperature and magnetic field (H) dependence of the magnetization (M) and magnetic susceptibility χ ($= M/H$). These investigations reveal that in addition to the presence of Co needles of diameter $d \approx 1$ nm, Co is also present as CoO and a complex cobalt silicate hydroxide with the formula $Co_3(Si_2O_5)_2(OH)_2$. The magnetization is dominated by large values from the Co needles. These experimental results and their discussion are presented in the following section.

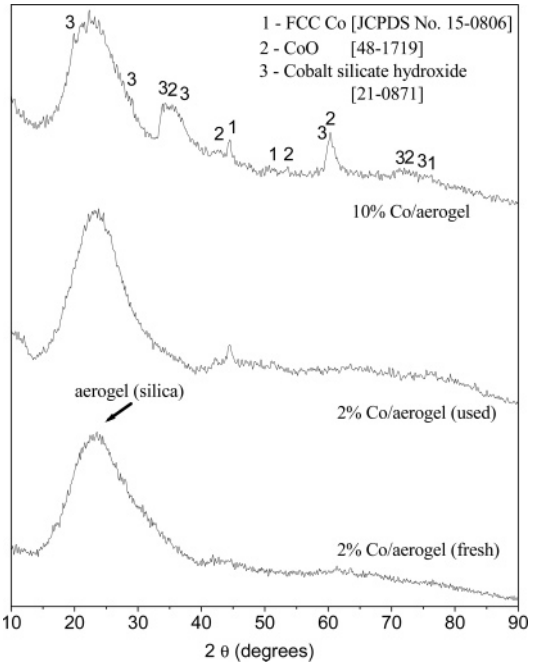

Figure 1. Room-temperature XRD patterns of the 10% Co/aerogel and 2% Co/aerogel samples. The identified phases are noted. The broad peak near $2\theta \approx 22°$ is due to silica aerogel.

Results and Discussion

Structure and Morphology. The procedures for the synthesis of the 10%Co/aerogel sample are described in ref

* Corresponding author. E-mail: mseehra@wvu.edu.
[†] West Virginia University.
[‡] University of Utah.
[§] University of Kentucky.

(1) Dunn, B. C.; Cole, P.; Covington, D.; Webster, M. C.; Pugmire, R. J.; Ernst, R. D.; Eyring, E. M.; Shah, N.; Huffman, G. P. *Appl. Catal., A* **2005**, *278*, 233.

10.1021/cm051033m CCC: $30.25
Published on Web 08/24/2005

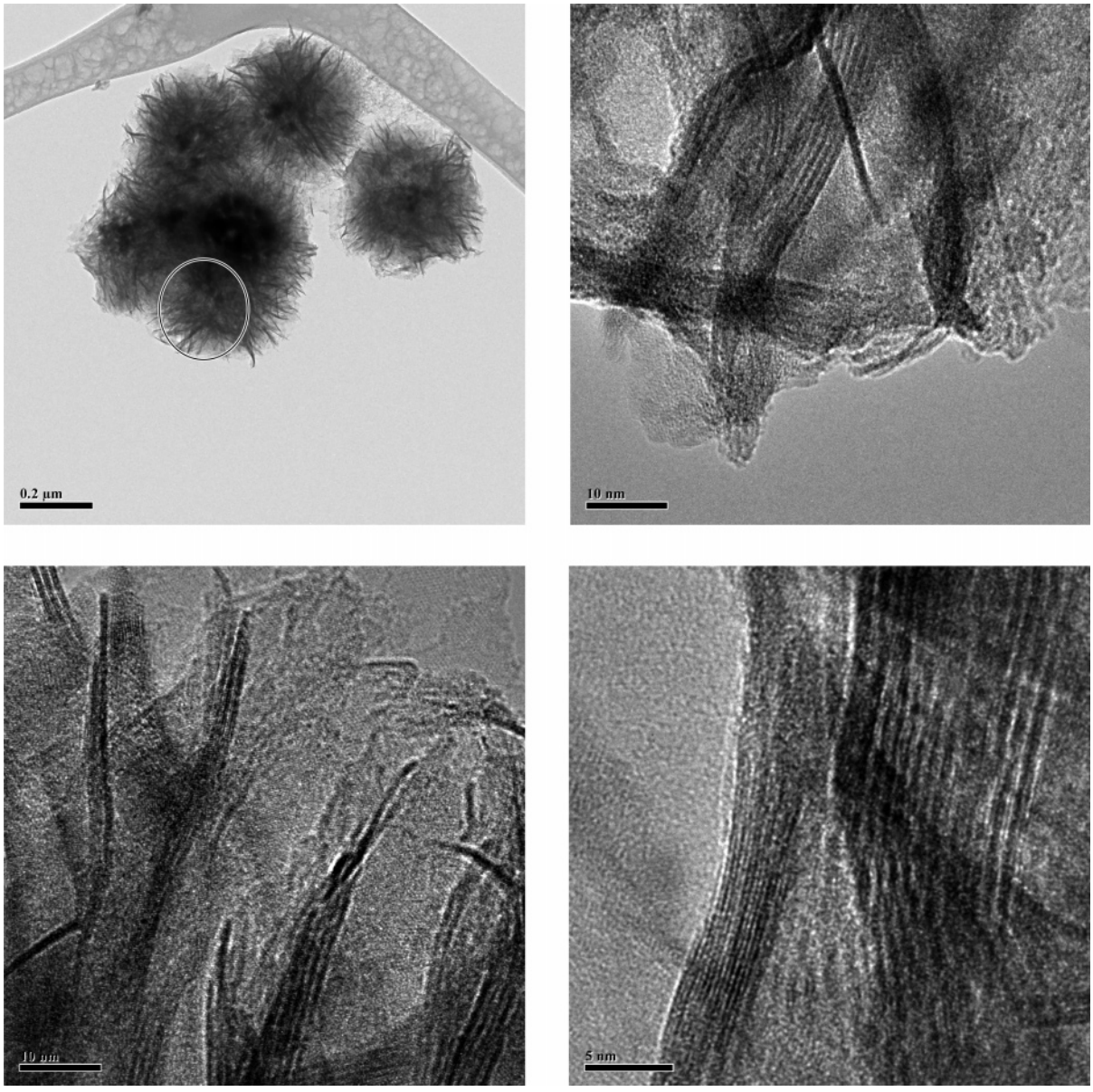

Figure 2. TEM micrographs of the 10% Co/aerogel sample with different magnifications.

1. The precursor used for Co loading was $Co(NO_3)_2 \cdot 6H_2O$, which under processing conditions changes to Co_3O_4. The sample is reduced in H_2 gas at 500 °C for 4 h.[1] The XRD pattern of the as-received sample is shown in Figure 1, using the Cu K_α radiation ($\lambda = 0.15418$ nm). The expected peak positions for FCC Co, CoO, and $Co_3(Si_2O_5)_2(OH)_2$ are also noted in Figure 1. The broad peak near $2\theta \approx 22°$ is due to the SiO_2 aerogel support. It is evident that for the 10% loading, Co has reacted with the support forming the silicate, whereas the presence of CoO is likely due to partially reduced Co_3O_4 since the reduction step may follow the sequence $Co_3O_4 \rightarrow CoO \rightarrow Co$.[2] As we shall see later, partial oxidation of Co to CoO after exposure to air can be ruled out from magnetic measurements. For the purpose of comparison, we have also shown the XRD patterns of 2% Co (fresh and used) samples in Figure 1 where there is no evidence of the presence of a silicate.

The TEM micrographs for the 10% Co/aerogel sample are shown in Figure 2. The presence of needlelike features with diameter ≈1 nm is quite evident, which we will show consist primarily of elemental Co. The presence of CoO and the cobalt silicate noted previously cannot be identified in the TEM pictures.

Magnetic Characterization. To further characterize the different phases, detailed *M* versus *H* and *M* versus *T* measurements were carried out using a commercial Superconducting Quantum Interference Device (SQUID) magnetometer. The data presented here are corrected for the diamagnetic contribution of the sample holder, as described in ref 3. For ZFC (zero-field cooling), the sample is cooled in zero magnetic field to the lowest temperature, a measuring field (200 Oe) is then applied, and the data are taken with increasing temperature after stabilizing at each point. After reaching the highest temperature (350 K), the data are then

(2) Ernst, B.; Libs, S.; Chaumette, P.; Kiennemann, A. *Appl. Catal., A* **1999**, *186*, 145.

(3) Seehra, M. S.; Babu, V. S.; Manivannan, A. J.; Lynn, W. *Phys. Rev. B.* **2000**, *61*, 3513.

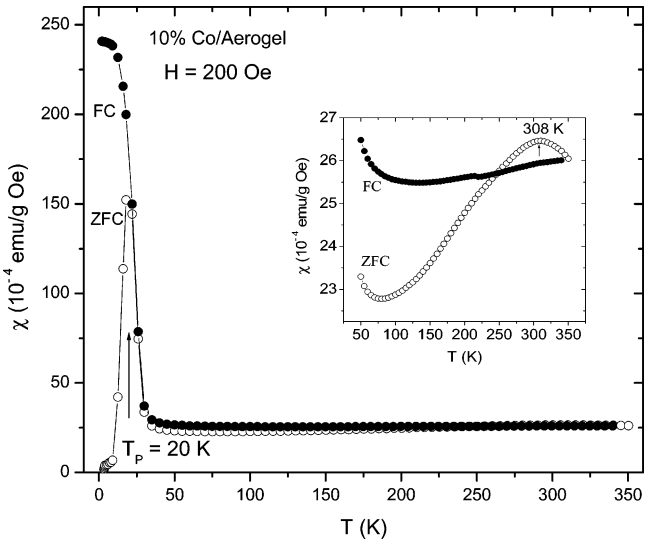

Figure 3. Temperature dependence of the magnetic susceptibility χ for the ZFC and FC cases. The inset shows an expanded version of the data for higher temperatures. The lines joining the data points are for visual aid.

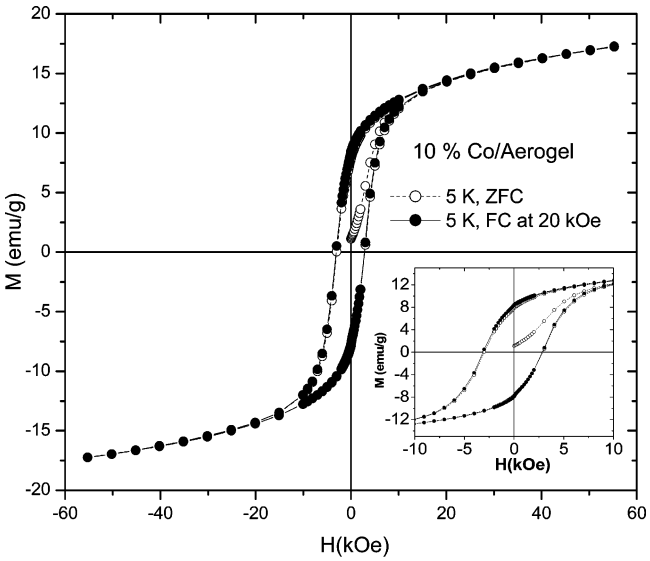

Figure 4. Hysteresis loops measured at 5 K under ZFC and FC at 20 kOe. The inset shows the expanded version for lower fields. The lines joining the data points are for visual aid.

taken with decreasing temperature, referred to here as the FC (field cooled) case.

The temperature variation of the magnetic susceptibility χ (= M/H)) for the 10% Co/aerogel sample in the ZFC and FC modes is shown in Figure 3. In the inset of Figure 3, the data are shown on an expanded scale for the higher temperatures. The peak near 308 K can be associated with paramagnetic to antiferromagnetic ordering of CoO,[4] knowing that there is some evidence for the presence of CoO from XRD also (Figure 1). At lower temperatures, the ZFC data peak near ≈20 K, below which there is a bifurcation of the ZFC and FC data. This bifurcation can be associated with nanoparticle magnetism,[3,5] in this case Co needles with $d \approx$ 1 nm as shown in Figure 2.[6] Thus, from the data in Figure 3, the presence of nanosize Co and CoO is indicated.

To determine whether Co and CoO represent a composite system, we measured the hysteresis loop of the sample at 5 K under two conditions: (i) ZFC and (ii) FC in 20 kOe. Since Co is a ferromagnet (F) and CoO an antiferromagnet (AF), the hysteresis loop would have shifted to the negative side if Co/CoO were a composite system because of the well-known exchange-bias phenomenon at a F/AF interface.[7,8] In the data shown in Figure 4, no significant shift of the loop is observed, suggesting that Co and CoO are separate entities in the sample. This is an important result of this work.

The shape and parameters of the loop (coercivity H_c, remanence M_r, and the high-field magnetization M_s) change considerably with sample temperature. In Figure 5, we show hysteresis loops at selected temperatures of 5, 25, 50, and 350 K. Similar data were taken at other temperatures, and temperature variations of the loop parameters viz. H_c, M_r ($H = 0$), M_s ($H = 20$ kOe), and M_r/M_s are shown in Figure 6. Note that M_r, M_r/M_s, and H_c show minimum values near $T_p = 20$ K. For $T > T_p$, M_s decreases rapidly, whereas the remanence M_r maintains a small nearly temperature-independent value up to 350 K.

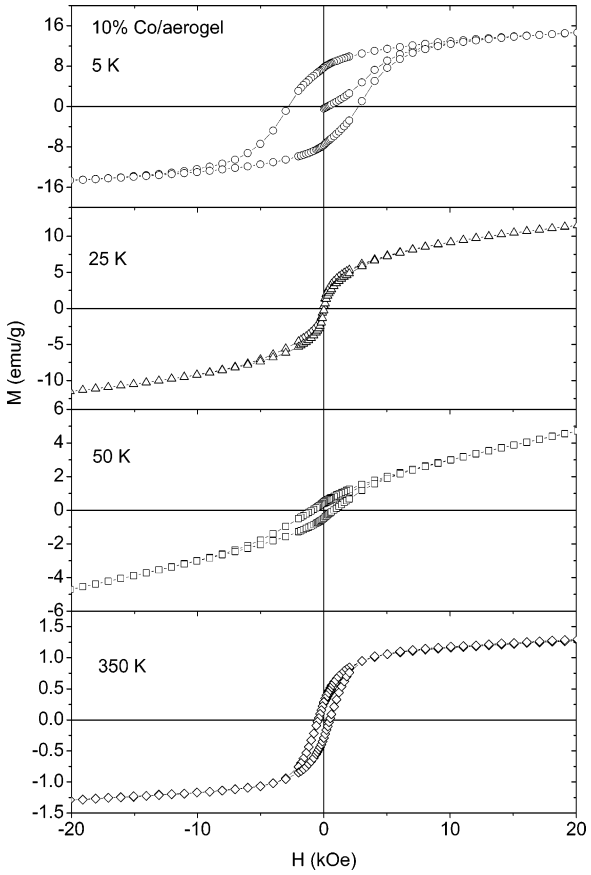

Figure 5. Hysteresis loops shown at selected temperatures of 5, 25, 50, and 350 K. Note different ordinate scales for different temperatures.

What is the interpretation of the temperature dependence of the loop parameters (Figure 6) in terms of the cobalt content of this sample? It is suggested that most of the observations are due to Co nanoneedles oriented randomly

(4) Seehra, M. S.; Silinsky, P. *Solid State Commun.* **1978**, *31*, 183.
(5) See the review by Berkowitz, A. E.; Takano, K. *J. Magn. Magn. Mater.* **1999**, *200*, 552 and references therein.
(6) Murray, C. B.; Sun, S.; Doyle, H.; Betley, T. *MRS Bull.* **2001**, *26*, 985.
(7) Meiklejohn, W. H.; Bean, C. P. *Phys. Rev.* **1956**, *102*, 1413 and ibid *J. Appl. Phys.* **1962**, *33*, 1398.
(8) See the review by Nogues, J.; Schuller, I. K. *J. Magn. Magn. Mater.* **1999**, *192*, 203.

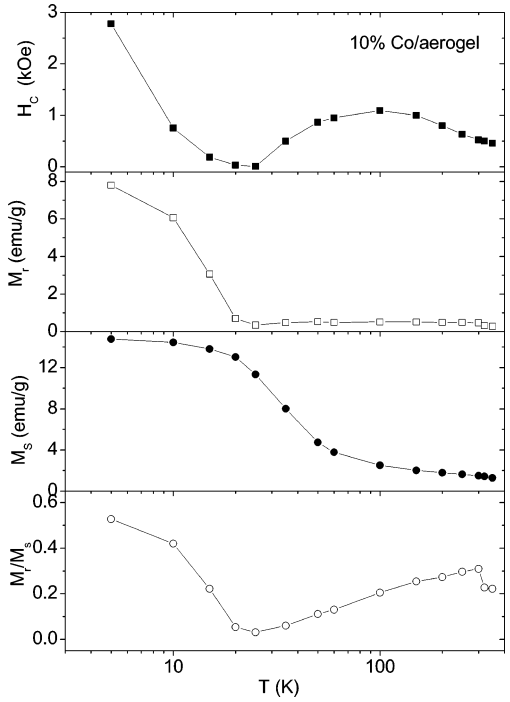

Figure 6. Temperature dependence of the hysteresis loop parameters viz. coercivity H_c, remanance M_r, high field magnetization M_s, and ratio M_r/M_s. Lines through the points are for visual aid.

with respect to the applied field H. For the Co nanoneedles, the shape anisotropy is the dominant source of anisotropy that makes the magnetic moments align parallel to the axis of the needles.[9,10] The measured M_s value for our sample at 5 K is ≈14 emu/g. For pure Co, the reported[11] M_s is ≈1446 emu/cm^3. Using density $\rho = 8.9$ g/cm^3 for Co, M_s for Co is 162.5 emu/g. Therefore, the calculated percentage of Co in the 10% Co/aerogel sample is 14/162.5 = 8.6%. This magnitude is close to the nominal 10% Co concentration. Thus, the measured magnetization can be explained by the presence of Co nanoneedles, the magnetization of CoO, and the cobalt−silicate being negligible comparatively.

The squareness of the loop defined by M_r/M_s for a single domain ellipsoidal particle can vary from 1 for H parallel to the easy axis to zero for H perpendicular to the easy axis, yielding an average magnitude of ≈0.5 for randomly oriented particles with respect to H.[12] The magnitude of M_r/M_s observed in Figure 6 is ≈0.5 at 5 K approaching near zero at $T_p \approx 20$ K. For $T > T_p$, M_r/M_s again increases, approaching the magnitude of ≈0.3 at 300 K. Since for $T < T_p$, magnetization is blocked from thermal fluctuations,[3,4] the system behaves as an ordered system, and all the measured properties are explained by randomly oriented Co nanoneedles, with the magnetization aligned parallel to the axis of the needles. The large magnitude of the coercivity H_c = 3000 Oe at 5 K is due to the large shape anisotropy of very thin needles since it is known that for Co nanowires, H_c increases as the diameter decreases.[9,10] Why H_c and M_r/M_s again increase after approaching near zero values at $T = T_p$ as expected for a superparamagnet[3,5,6] may be due to nanoneedles with much smaller aspect ratios that may have a higher T_p. Support for this comes from a recent paper on $Cu_{90}Co_{10}$ granular alloys where Nunes et al.[13] have reported a similar broad hump in H_c above T_p. This was explained on the basis of a size distribution of the nanoparticles (leading to a size distribution of the blocking temperatures) and interparticle interaction. The nanoneedles with higher T_p values and clustering of the nanoneedles observed here (Figure 2) leading to interparticle interaction may then be responsible for the observed hump in H_c (Figure 6). The magnetic properties of the cobalt silicate hydroxide $Co_3(Si_2O_5)_2(OH)_2$ observed in the XRD patterns (Figure 1) in our sample are also largely unknown. Finally, it is noted that besides the reviews of refs 6 and 9, which include extensive discussions of the magnetic properties of Co nanoparticles, there have been several recent reports on the synthesis and properties of Co nanoparticles of various shapes and sizes.[14−17] The results discussed here have taken into account any relevant information from these sources.

Conclusion

The experimental results presented here on the nominal 10% Co/aerogel FT catalyst have shown the presence of not only Co nanoneedles but also the presence of unreduced CoO and a cobalt silicate hydroxide $Co_3(Si_2O_5)_2(OH)_2$. This use of three complimentary techniques (XRD, TEM, and magnetometry) for determining the characteristics of the different phases of Co in this system is an important contribution of this work. The presence of the unreduced cobalt explains why the FT activity of this 10% Co/aerogel catalyst is about equal to that of the 6% Co/aerogel sample. Some very interesting magnetic properties of the Co nanoneedles present in this sample are also reported.

Acknowledgment. This work was supported in part by the U.S. Department of Energy through the Consortium for Fossil Fuel Science (Contract DE-FC26-02NT41594).

CM051033M

(9) Fert, A.; Piraux, L. *J. Magn. Magn. Mater.* **1999**, *200*, 338.
(10) Ferre, R.; Ounadjela, K.; George, J. M.; Piraux, L.; Dubois, S. *Phys. Rev. B* **1997**, *56*, 14066.
(11) Kittel, C. *Introduction to Solid State Physics*, 7th ed.; John Wiley: New York, 1996; pp 449 and 24.
(12) Stoner, E. C.; Wohlfarth, E. P. *Philos. Trans. R. Soc. London, Ser. A* **1948**, *240*, 599.
(13) Nunes, W. C.; Folly, W. S. D.; Sinnecker, J. P.; Novak, M. A. *Phys. Rev. B* **2004**, *70*, 014419.
(14) Darques, M.; Piraux, L.; Encinas, A. Bayle-Guillemand, P.; Popa, A.; Ebels, U. *Appl. Phys. Lett.* **2005**, *86*, 072508.
(15) Luo, H.; Wang, D.; He, J.; Lu, Y. *J. Phys. Chem. B* **2005**, *109*, 1919.
(16) Puntes, V. F.; Krishnan, K. M.; Alivisatos, A. P. *Science* **2001**, *291*, 2115.
(17) Luis, F.; Torres, J. M. Garcia, L. M. Bartolome, J.; Stankiewicz, J.; Petroff, F.; Fetter, F.; Maurice, J. L.; Vaures, A. *Phys. Rev. B* **2002**, *65*, 094409.